

Kinetic Studies of AMP-Dependent Phosphorolysis of Amylopectin Catalyzed by Phosphorylase *b* on a 27 MHz Quartz-Crystal Microbalance

Hidekazu Nishino, Akiko Murakawa, Toshiaki Mori, and Yoshio Okahata*

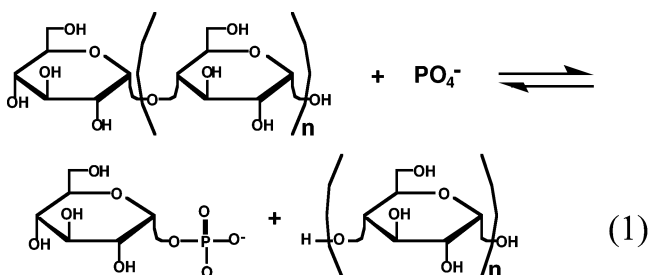
Contribution from the Department of Biomolecular Engineering, Frontier Collaborative Research Center, Tokyo Institute of Technology and CREST, Japan Science and Technology Corporation (JST), 4259 Nagatsuta, Midori-ku, Yokohama, 226-8501, Japan

Received June 10, 2004; E-mail: yokahata@bio.titech.ac.jp

Abstract: Catalytic cleavage reactions of phosphorylase *b* were monitored directly on an amylopectin-immobilized 27 MHz quartz-crystal microbalance (QCM). When the inactivated phosphorylase *b* was injected into a phosphate buffer solution of amylopectin-immobilized QCM (method A), the binding of the enzyme to amylopectin was observed as a frequency decrease (mass increase). Then, when AMP (adenosine monophosphate) was added to activate the enzyme, the frequency gradually increased (mass decreased) due to the phosphorolysis of amylopectin in the presence of phosphates as buffers. When the AMP-activated phosphorylase *b* was employed (method B), the continuous reaction was observed which includes both the mass increase due to the enzyme binding to amylopectin at first and then the following mass decrease due to the phosphorolysis by the AMP-activated enzyme. All kinetic parameters for the enzyme binding to the substrate (binding and dissociation rate constants, k_{on} and k_{off} , and dissociation constant, K_d), the AMP binding to the enzyme as activator (K_{AMP}), the catalytic rate constant (k_{cat}) were obtained from curve fittings of time-courses of frequency (mass) changes. The obtained kinetic parameters were compared with those from Michaelis–Menten kinetics.

Introduction

Glycogen phosphorylase (EC 2.4.1.1) catalyzes the phosphorolysis of α -1,4 glucosidic linkages from the nonreducing termini of glycogen to produce a glucose-1-phosphate (G-1P).¹



Phosphorylase *b* (from rabbit muscle) is a typical glycogen phosphorylase for amylopectin in the presence of excess phosphate anions, and generally exists as an inactive T-state conformation in the liver, which is changed to the active R-state conformation by AMP (adenosine monophosphate) binding.^{2–6}

Thus, the activity of phosphorylase *b* can be regulated by the addition of AMP. The cleavage of α -1,4 glucosidic linkages has been studied using the radioisotope-labeled phosphoric acids to follow the production of glucose-1-phosphate in solution. Because detection of ES intermediate is generally difficult, enzyme reactions are usually studied using a steady-state approach in the bulk solution, in which the concentration of the enzyme–substrate (ES) complex is hypothesized to be nearly constant through the out the course the of the concentration of the was generally difficult.^{7–9} If the formation and decomposition of the ES complex can be followed directly during the reaction, then more accurate kinetic constants might be obtained.

We have previously reported that a 27-MHz quartz-crystal microbalance (QCM) is a useful tool to directly and quantitatively detect various molecular recognitions such as DNA–DNA hybridization,¹⁰ DNA–protein interactions,¹¹ enzyme reactions on DNA,¹² RNA–peptide interactions,¹³ and glycolipid–protein

- (1) Madsen, N. B. *A Study of Enzymes*; Kuby, S. A., Ed.; CRC Press: Boca Raton, 1991, Vol. II, p 139.
- (2) Martin, J. L.; Johnson, L. N.; Withers, S. G. *Biochemistry* **1990**, *29*, 10745–10757.
- (3) Browner, M. F.; Fletterick, R. J. *Trends Biochem. Sci.* **1992**, *17*, 66–71.
- (4) McLaughlin, P. J.; Stuart, D. I.; Klein, H. W.; Oikonomakos, N. G.; Johnson, L. N. *Biochemistry* **1984**, *23*, 5862–5873.
- (5) Barford, D.; Schwabe, J. W. R.; Oikonomakos, N. G.; Acharya, K. R.; Hajdu, J.; Papageorgiou, A. C.; Martin, J. L.; Knott, J. C. A.; Vasella, A.; Johnson, L. N. *Biochemistry* **1988**, *27*, 6733–6741.

- (6) Palm, D.; Klein, H. W.; Schinzel, R. S.; Bucher, M.; Helmreich, E. J. M. *Biochemistry* **1990**, *29*, 1099–1107.
- (7) Guissani, A. *Eur. J. Biochem.* **1977**, *79*, 233–243.
- (8) Segel, H. *Enzyme Kinetics*; John Wiley & Sons: New York, 1975.
- (9) Kuby, S. A., Ed. *A Study of Enzymes Volume I*; CRC Press: Boca Raton, 1991.
- (10) (a) Okahata, Y.; Matsunobu, Y.; Ijiro, K.; Mukai, M.; Murakami, A.; Makino, K. *J. Am. Chem. Soc.* **1992**, *114*, 4, 8299–8300. (b) Okahata, Y.; Kawase, M.; Niikura, K.; Ohtake, F.; Furusawa, H.; Ebara, Y. *Anal. Chem.* **1998**, *70*, 1288–1296.
- (11) (a) Niikura, K.; Nagata, K.; Okahata, Y. *Chem. Lett.* **1996**, 863–864. (b) Okahata, Y.; Niikura, K.; Sugiura, Y.; Sawada, M.; Morii, T. *Biochemistry* **1998**, *37*, 5666–5672. (c) Matsuno, H.; Niikura, K.; Okahata, Y. *Biochemistry* **2001**, *40*, 3615–3622. (d) Furusawa, H.; Kitamura, Y.; Hagiwara, N.; Tsurimoto, T.; Okahata, Y. *ChemPhysChem* **2002**, 446–448.

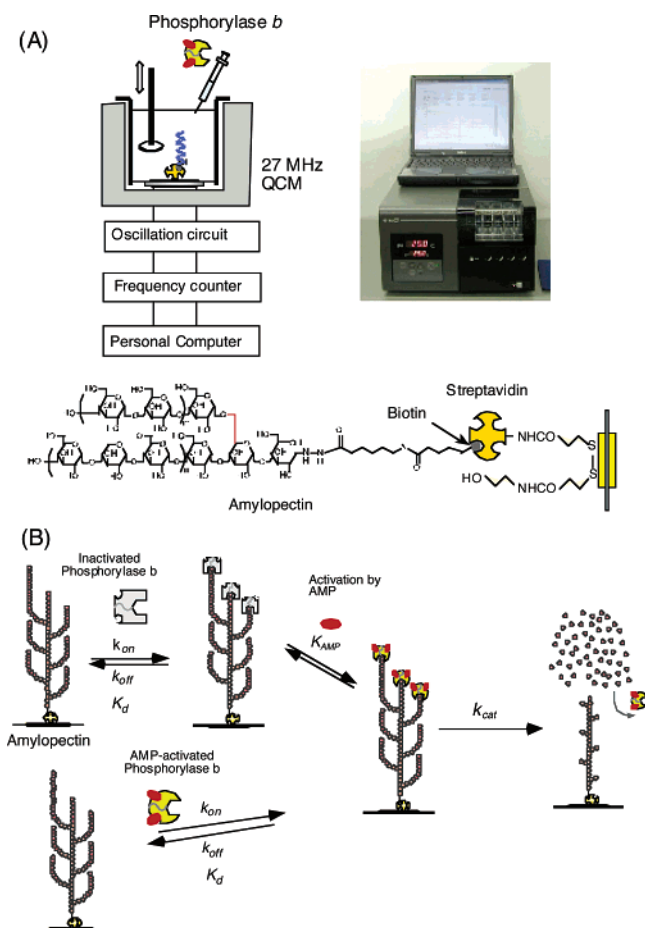


Figure 1. (A) Experimental setup (Affinix Q⁴) for phosphorolysis reactions on an amylopectin-immobilized 27 MHz quartz-crystal microbalance (QCM) in phosphate buffer solution, and (B) the reaction schemes and kinetic parameters obtained in this work.

interactions.¹⁴ The 27 MHz QCM is a very sensitive mass measuring device in aqueous solutions, and its resonance frequency is proved to decrease linearly with increasing mass on the QCM electrode at the nanogram level.^{10–16}

We report that all kinetic processes of phosphorylase *b* for the amylopectin substrate, such as enzyme binding (mass increase), the activation of enzymes by AMP binding, and the phosphorolysis of substrates (mass decrease), which were analyzed by following the frequency (mass) changes of the amylopectin-immobilized 27 MHz QCM (Figure 1). In the binding process of phosphorylase *b* to the nonreducing termini of amylopectin, the binding (k_{on}) and dissociation (k_{off}) rate constants, and dissociation constant (K_{d}) of the enzyme–substrate complex could be obtained. In the following activation step by AMP, the Michaelis constant for AMP (K_{AMP}) to the enzyme could be obtained. In the phosphorolysis step, the catalytic rate constant (k_{cat}) was obtained from the initial rate

of phosphorolysis. The 27 MHz QCM used in this study has a sensitivity of 0.62 ng cm^{-2} of mass change per 1 Hz of frequency decrease.^{10–14} This sensitivity is large enough to sense both the binding of enzyme and the cleavage of amylopectin (Figure 1B).

Experimental Section

Materials. Phosphorylase *b* from rabbit muscle [EC 2.4.1.1], biotinamidocaproylhydrazide, streptavidin, and AMP were purchased from SIGMA-Aldrich (Tokyo). Amylopectin was from Hayashibara Co. (Tokyo, Japan). All other reagents were purchased from Nacalai Tesque Co. (Kyoto) and used without further purification.

27 MHz QCM Setup and its Calibration. An Affinix Q⁴ was used as a QCM instrument (Initium Co. Ltd, Tokyo, <http://www.initium2000.com>) having four 500 μL cells equipped with a 27 MHz QCM plate (8 mm diameter of a quartz plate and an area of 4.9 mm² of Au electrode) at the bottom of the cell and the stirring bar with the temperature controlling system.¹⁸ The Sauerbrey's equation¹⁵ was obtained for the AT-cut shear mode QCM

$$\Delta F = -\frac{2F_0^2}{A\sqrt{\rho_q\mu_q}} \Delta m \quad (2)$$

where ΔF is the measured frequency change [Hz], F_0 the fundamental frequency of the quartz crystal prior to a mass change [27×10^6 Hz], Δm the mass change [g], A the electrode area [0.049 cm^2], ρ_q the density of quartz [2.65 g cm^{-3}], and μ_q the shear modulus of quartz [$2.95 \times 10^{11} \text{ dyn cm}^{-2}$]. Calibration of the 27 MHz QCM was performed such that a frequency decrease of 1 Hz corresponded to a mass increase of $0.62 \pm 0.1 \text{ ng cm}^{-2}$ on the QCM electrode, as described previously.^{10–14} The noise level of the 27 MHz QCM was ± 1 Hz in buffer solutions at 25 °C, and the standard deviation of the frequency was ± 2 Hz for 2 h in buffer solutions at 25 °C.

Preparation of Amylopectin-Immobilized QCM Plates. The biotinylated-amylopectin (average Mw: $100 \pm 50 \text{ kDa}$) was prepared as previously described.^{17,18} by the reaction of the reducing end of amylopectin with biotinamidocaproylhydrazide (Figure 1A). The biotinylated amylopectin was anchored on a streptavidin-immobilized QCM. The immobilized amount of biotinylated amylopectin was determined to be $620 \pm 20 \text{ ng cm}^{-2}$ (ca. 6.2 pmol cm^{-2}). This corresponds to approximately 70% coverage of the streptavidin binding pockets.

Enzyme Reactions on Amylopectin-immobilized QCM Plates. An amylopectin-immobilized QCM plate was soaked in 0.5 mL of buffer solution containing 50 mM phosphate (pH 6.8) and 200 mM NaCl, until the resonance frequency reached a steady state. Frequency changes after the addition of enzyme and/or AMP solutions into the cell were followed with time. The solution was vigorously stirred to avoid any effect of slow diffusion of enzymes and AMP. The stirring did not affect the stability and magnitude of frequency changes.

Results

In Situ Monitoring of Amylopectin Cleavage Reactions by Phosphorylase *b*. Figure 2 shows typical frequency changes of the amylopectin-immobilized QCM as a function of time, responding to the addition of phosphorylase *b* and/or AMP in the buffer solution containing excess amount of phosphate ions (50 mM). In method A, the inactivated phosphorylase *b* was injected (13.4 nM) and this corresponded to a gradual frequency

- (12) (a) Niikura, K.; Matsuno, H.; Okahata, Y. *J. Am. Chem. Soc.* **1998**, *120*, 8537–8538. (b) Niikura, K.; Matsuno, H.; Okahata, Y. *Chem. Eur. J.* **1999**, *5*, 1609–1616. (c) Matsuno, H.; Niikura, K.; Okahata, Y. *Chem. Eur. J.* **2001**, *7*, 3305–3312. (d) Matsuno, H.; Okahata, Y. *Chem. Commun.* **2002**, 470–471.
- (13) Furusawa, H.; Murakawa, A.; Fukusho, S.; Okahata, Y. *ChemBioChem* **2003**, *217–220*.
- (14) (a) Ebara, Y.; Okahata, Y. *J. Am. Chem. Soc.* **1994**, *116*, 11209–11212. (b) Ebara, Y.; Itakura, K.; Okahata, Y. *Langmuir* **1996**, *12*, 5165–5170. (c) Ebara, Y.; Mizutani, K.; Okahata, Y. *Langmuir* **2000**, *16*, 2416–2418.
- (15) Sauerbrey, G. *Z. Z. Physik* **1959**, *155*, 206–222.
- (16) Janshoff, A.; Galla, H.-J.; Steinem, C. *Angew. Chem., Int. Ed.* **2000**, *39*, 4004–4006.

- (17) (a) Shinohara, Y.; Sota, H.; Gotoh, M.; Hasebe, M.; Tosu, M.; Nako, J.; Hasegawa, Y.; Shiga, M. *Anal. Chem.* **1996**, *68*, 2573–2579. (b) Sun, X.-L.; Faucher, K. M.; Houston, M.; Grande, D.; Chaikof, E. L. *J. Am. Chem. Soc.* **2002**, *124*, 7258–7259.
- (18) Nishino, H.; Nihira, T.; Mori, T.; Okahata, Y. *J. Am. Chem. Soc.* **2004**, *126*, 2264–2265.

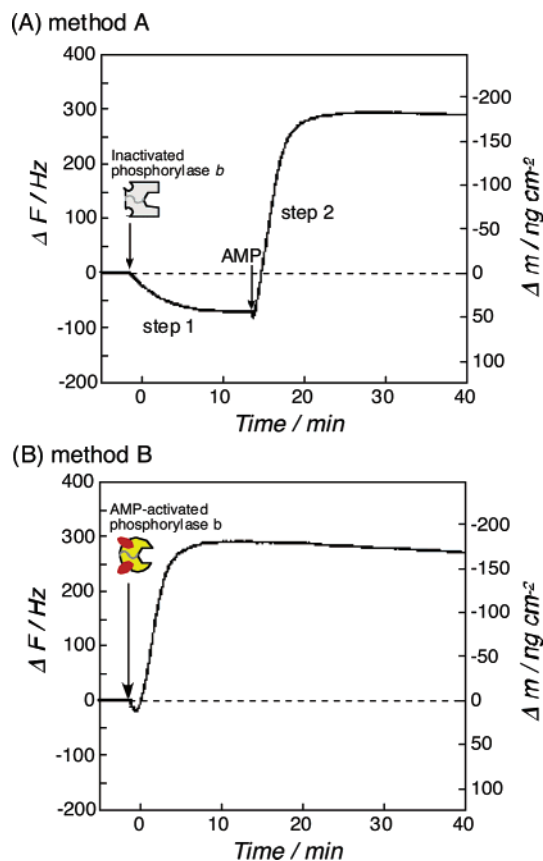


Figure 2. Typical time courses of frequency changes of the amylopectin-immobilized 27 MHz QCM, responding to the addition of (A) the inactivated phosphorylase *b* and then AMP, and (B) the AMP-activated phosphorylase *b* in the presence of excess AMP. Immobilized amount of amylopectin = $620 \pm 20 \text{ ng cm}^{-2}$ (6.2 pmol cm^{-2}) on a QCM plate (4.9 mm^2 Au electrode), [phosphorylase *b*] = 13.4 nM , [AMP] = 2 mM , 50 mM phosphate buffer, pH 6.8, 200 mM NaCl, $25 \text{ }^\circ\text{C}$.

decrease for 15 min due to the slow binding of the enzyme to amylopectin (step 1). After the frequency change reached equilibrium, excess AMP (2 mM) was injected to the solution. The frequency rapidly increased (mass decreased) to a constant value ($-180 \pm 20 \text{ ng cm}^{-2}$ over the starting zero point) within a few minutes (step 2). This indicates that phosphorylase *b* could bind to amylopectin even as the inactivated form and the activated enzyme by AMP could phosphorolyse amylopectin on the QCM (see eq 1). In method B, when the AMP-activated enzyme was injected in the presence of excess AMP, the frequency decreased (mass increased) slightly at first and then spontaneously increased (mass decreased) and reached the same mass decrease obtained by method A. This continuous frequency change shows that the binding of AMP-activated enzyme to the substrate (mass increase) was followed by phosphorolysis (mass decrease).

The mass decrease from the starting zero point was $-180 \pm 20 \text{ ng cm}^{-2}$, which corresponds to 30% of the immobilized amylopectin (620 ng cm^{-2} , ca. 6.2 pmol cm^{-2}). The amylopectin is a branched α -1,4 glucan with α -1,6 glucosidic linkages at branched points as shown in Figure 1A. It is known that AMP-activated phosphorylase *b* can phosphorolyse amylopectin from the nonreducing termini of α -1,4 glucosidic linkages, but cannot phosphorolyse the α -1,6 branched points of amylopectin.¹ Thus, the mass decrease of $180 \pm 10 \text{ ng cm}^{-2}$ after phosphorolysis in both methods A and B indicates that the enzyme phospho-

rolyzed the branched α -1,4 glucosidic linkages of amylopectin and released these fragments.

Curve fittings of step 1 of method A enabled us to obtain (i) the binding and dissociation rate constants (k_{on} and k_{off} , respectively) and dissociation constants ($K_{\text{d}} = k_{\text{off}}/k_{\text{on}}$) of inactivated phosphorylase *b* to substrate, (ii) from step 2 of method A, we obtained the catalytic phosphorolysis rate constant (k_{cat}) and Michaelis constant for AMP (K_{AMP}) of the AMP-activated enzyme, and (iii) from method B, we determined the binding and phosphorolysis rate constants (k_{on} , k_{off} , K_{d} , and k_{cat}) of AMP-activated enzyme.

Effect of Enzyme Concentrations on Amylopectin-Binding. The binding of inactivated phosphorylase *b* to the nonreducing end of amylopectin is described by eq 3 (step 1 of Figure 2A). We followed the formation of *ES* complex over time on the QCM. At time *t*, the mass of *ES* is given by eqs 4–6, where *E* indicates the inactivated-phosphorylase *b*, *S* indicates amylopectin, and $[E]_0 \gg [S]_0$.



$$[ES]_t = [ES]_{\text{max}} \{1 - \exp(-t/\tau)\} \quad (4)$$

$$\Delta m_t = \Delta m_{\text{max}} \{1 - \exp(-t/\tau)\} \quad (5)$$

$$\tau^{-1} = k_{\text{on}}[E]_0 + k_{\text{off}} \quad (6)$$

Relaxation time (τ) associated with enzyme binding is calculated from curve fittings of the QCM frequency decrease in step 1. When binding experiments were carried out at different concentrations of enzyme, the binding and dissociation rate constants (k_{on} and k_{off}) of the enzyme to the substrate could be obtained from the slope and intercept of eq 6, respectively. The dissociation constant (K_{d}) was obtained from the ratio of k_{off} to k_{on} .

Figure 3A shows typical time courses for binding of inactivated phosphorylase *b* to amylopectin at various concentrations of enzyme (9.4 – 27 nM). Figure 3B shows the linear reciprocal plot of the relaxation time (τ) obtained from curve fittings of Figure 3A against concentrations of bound enzyme, which was calculated from the equilibrium binding amount of the enzyme at the step 1. From the slope and intercept of the plot, the binding and dissociation rate constants ($k_{\text{on}} = 1.6 \times 10^5 \text{ M}^{-1} \text{ s}^{-1}$ and $k_{\text{off}} = 1.9 \times 10^{-3} \text{ s}^{-1}$) were obtained, respectively. The results are summarized in Table 1. The $K_{\text{d}} = 1.2 \times 10^{-8} \text{ M}$ obtained from $k_{\text{off}}/k_{\text{on}}$ was very small despite the inactivated enzyme. This indicates that phosphorylase *b* can bind strongly to the nonreducing ends of α -1,4 glucosidic linkages of amylopectin even as the inactivated form.

In step 2 of Figure 3A, by the addition of AMP (2 mM), phosphorylase *b* was activated and the phosphorolysis (mass decrease) was observed at different enzyme concentrations. The final frequency increase was constant ($-180 \pm 20 \text{ ng cm}^{-2}$) and independent of enzyme concentration. The initial phosphorolysis rates (v_0), obtained from the initial frequency increase just after the addition of AMP, were plotted against the bound amounts of phosphorylase *b* calculated from step 1 of Figure 3A, and the results are shown in Figure 3C. The amylopectin cleavage rate increased linearly with the amount of bound

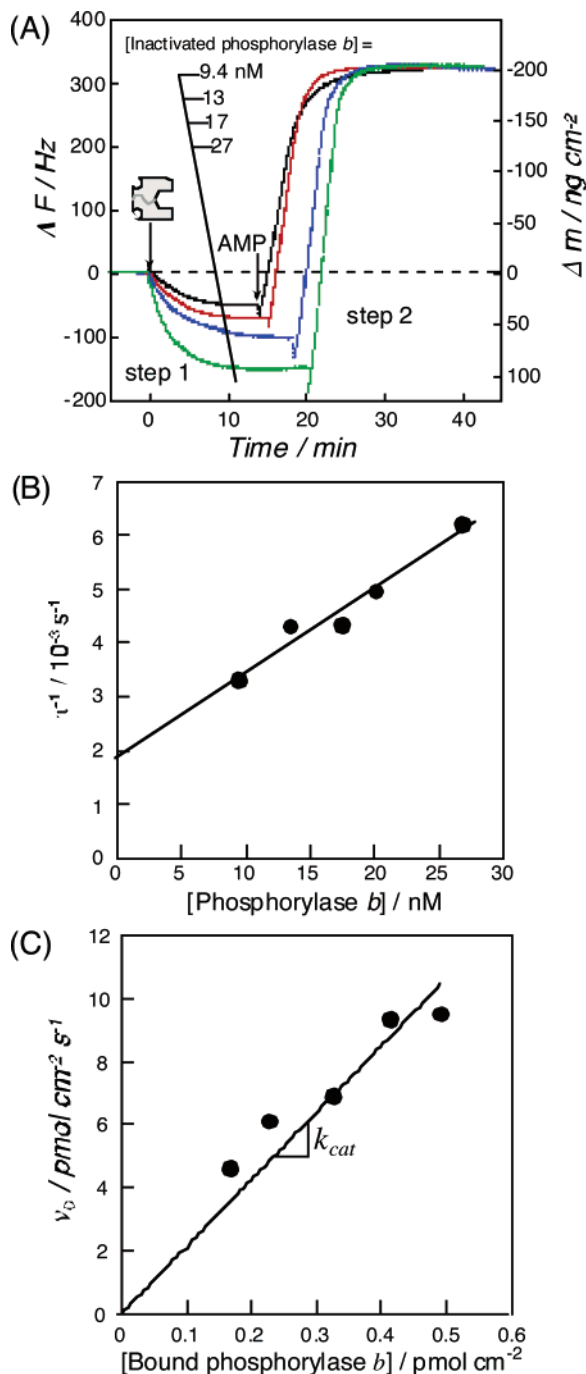


Figure 3. (A) Time courses of frequency decreases (mass increases) due to the inactivated phosphorylase *b* binding to the amylopectin and then frequency increases (mass decreases due to the phosphorolysis) by the addition of an excess AMP to activate the enzyme at different concentrations of the enzyme. ([Immobilized amylopectin] = 620 ng cm⁻², 50 mM phosphate, pH 6.8, 200 mM NaCl, 25 °C, [phosphorylase *b*] = 9.4–27 nM, [AMP] = 2 mM). (B) Linear reciprocal plots of the relaxation time (τ) against the inactivated phosphorylase *b* concentration according to eq 6 in the text. (C) Linear plot of initial phosphorolysis rates (v_0) just after the AMP injections against the concentrations of the bound phosphorylase *b* on amylopectin.

enzyme. The k_{cat} value obtained was 21 s⁻¹. The results are summarized in Table 1.

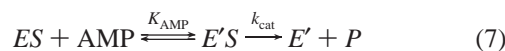
Effect of AMP Concentrations on Phosphorolysis. In method A, the *ES* complex was activated by the addition of AMP. Figure 4A shows the effect of AMP concentration on the rate of phosphorolysis at constant enzyme concentration

Table 1. Comparison of Kinetic Parameters of Phosphorolytic Reactions Catalyzed by Phosphorylase *b* from Rabbit Muscle^a

phosphorylase <i>b</i>	$k_{on}/10^3 \text{ M}^{-1} \text{ s}^{-1}$	$k_{off}/10^{-3} \text{ s}^{-1}$	$K_d/10^{-3} \text{ M}$	$K_m/10^{-6} \text{ M}$	k_{cat}/s^{-1}	$K_{AMP}/10^{-4} \text{ M}$
inactivated enzyme (method A)	160 ^b	1.9 ^b	12 ^b		21 ^c (12) ^d	1.0 ^d
AMP-activated enzyme (method B)	36 ^e	0.05 ^e	1.4 ^e		18 ^e	
in bulk solution				2.0 ^f	24 ^f	1.2 ^g

^a [Immobilized amount of amylopectin] = 620 ± 20 ng cm⁻² (6.2 pmol cm⁻²), [Phosphorylase *b*] = 9.4–27 nM, pH 6.8, 50 mM phosphate buffer, 200 mM NaCl, at 25 °C. ^b Obtained from eqs 5 and 6, and Figure 3B. ^c Obtained from Figure 3C. ^d Obtained from eq 9 and Figure 4C. ^e Obtained from eqs 11 and 12, and Figure 5B. ^f Obtained from Michaelis–Menten equations (refs 19 and 20). ^g Obtained from the radio-isotope method (ref 21).

([phosphorylase *b*] = 13.4 nM. Both the initial rate and the total amount of phosphorolysis increased with increasing AMP concentration. However, the total phosphorolysis amount reached constant values ($\Delta m = 180 \pm 20 \text{ ng cm}^{-2}$) even at the low AMP concentrations. The initial phosphorolysis rate (v_0) showed saturation behavior with increasing AMP concentrations (Figure 4B). This is simply expressed by the Michaelis–Menten equation (eq 7), where *ES* is the complex of the inactivated enzyme and amylopectin, *E'* is the AMP-activated enzyme, *P* is the product glucose-1-phosphate, K_{AMP} is the Michaelis constant for the AMP of the *ES* complex, and k_{cat} is the phosphorolysis rate constant. The *ES* complex was estimated to be 0.2 pmol cm⁻² from the frequency change after step 1 (eq 4). The initial rate of phosphorolysis is expressed by eq 8 and the Lineweaver–Burk plot (Figure 4C) is shown in eq 9. From the Lineweaver–Burk plot, $K_{AMP} = 100 \mu\text{M}$ and $k_{cat} = 12 \text{ s}^{-1}$ were obtained from the slope and intercept, respectively. The results are summarized in Table 1.



$$v_0 = \frac{V_{max}[AMP]_0}{K_{AMP} + [AMP]_0} \quad (8)$$

$$\frac{1}{v_0} = \frac{K_{AMP}}{V_{max}} \cdot \frac{1}{[AMP]_0} + \frac{1}{V_{max}} \quad (9)$$

Effect of Enzyme Concentration on Binding and Phosphorolysis. Figure 5A shows frequency changes as a function of time, when AMP-activated phosphorylase *b* was injected at different concentrations (9.4–27 nM) in the presence of 2 mM AMP. The frequency slightly decreased (mass increased) at first due to the binding of AMP-activated enzyme to substrate. Then the frequency continuously increased (mass decreased) due to the phosphorolysis of substrate on the QCM. Finally, the frequency reached a constant value ($-180 \pm 20 \text{ ng cm}^{-2}$ over the starting zero point) that was independent of enzyme concentration. Since amylopectin was immobilized in the amount of 620 ± 10 ng cm⁻² on the QCM plate, this indicates that ca. 30% of amylopectin was phosphorolyzed by the enzyme (This agrees with method A, see Figure 3A).

In sigmoidal curves of Figure 5A, the time dependence of Δm reflects both the formation of the *E'S* complex (eq 10) and

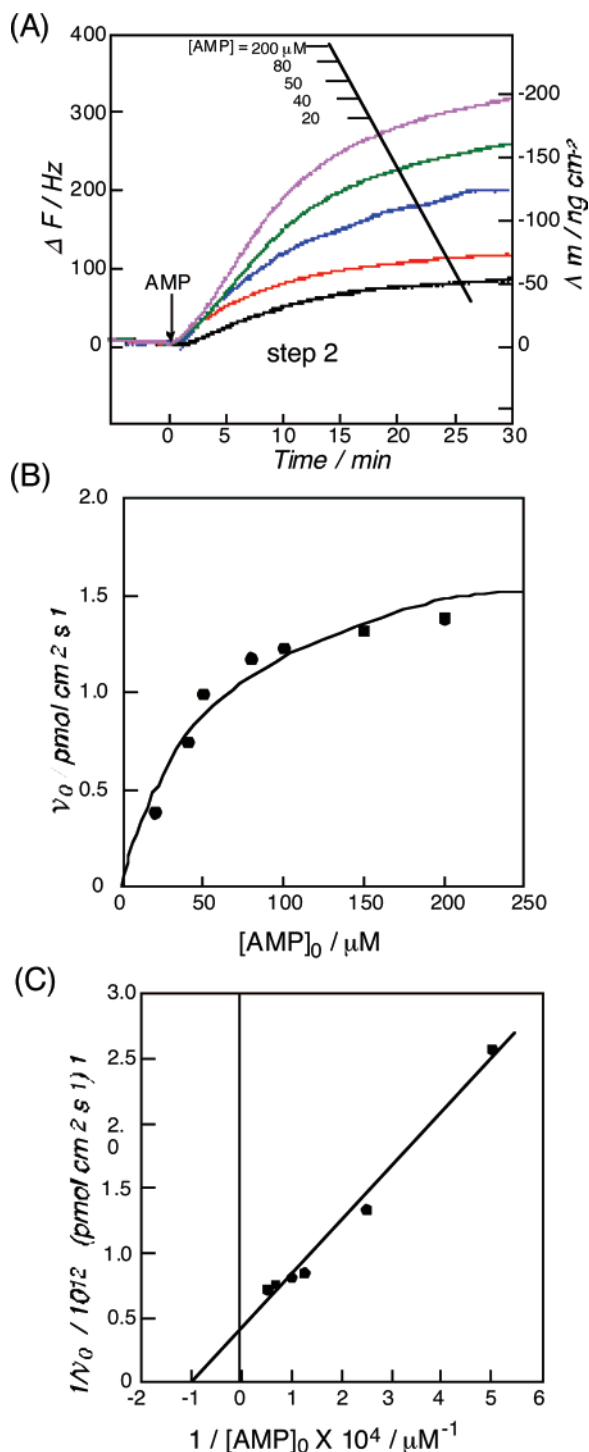


Figure 4. (A) Effect of AMP concentrations (20–200 μM) on the phosphorolysis started from the inactivated ES complex ([phosphorylase b] = 13.4 nM, $[ES]_0 = 0.2 \text{ pmol cm}^{-2}$, [immobilized amylopectin] = $620 \pm 20 \text{ ng cm}^{-2}$, 50 mM phosphate, pH 6.8, 200 mM NaCl, 25 $^\circ\text{C}$). (B) Michaelis–Menten saturation curve of the initial phosphorolysis rates (v_0) against AMP concentrations. (C) Lineweaver–Burk plots of (B).

the reduction of substrate (the formation of product, eq 11), where $E'S$ is the complex of the AMP-activated enzyme and substrate, P is the product (glucose-1-phosphate), and D_p is the degree of polymerization of amylopectin.

$$[E'S] = [E'S]_{\text{max}} \left(1 - e^{-\frac{t}{\tau}}\right) - [P] \left(1 - e^{-\frac{t}{\tau}}\right) \quad (10)$$

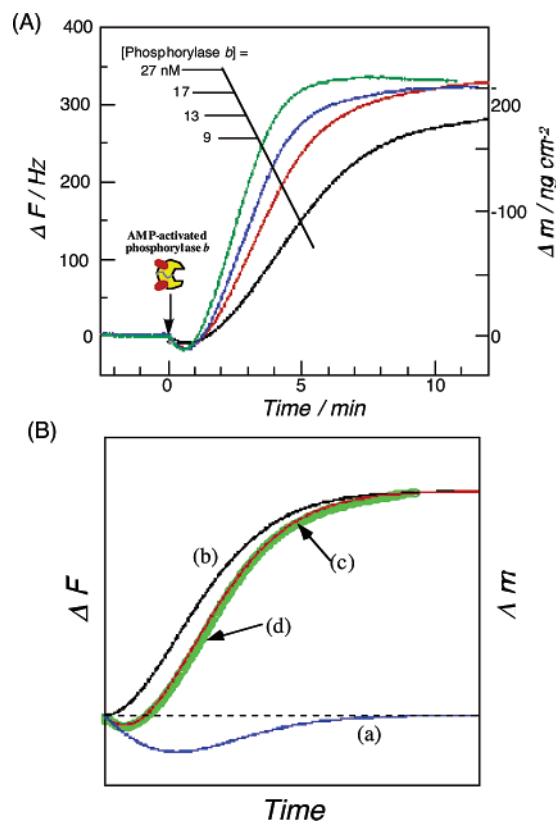


Figure 5. (A) Time courses of frequency changes of the amylopectin-immobilized QCM, responding to the addition of the AMP-activated phosphorylase b at 9.4–27 nM ([immobilized amylopectin] = 620 ng cm^{-2} , 50 mM phosphate buffer, pH 6.8, 200 mM NaCl, 25 $^\circ\text{C}$, [AMP] = 2 mM). (B) (a) the theoretical time dependence of $[E'S]$ as shown in eq 10 in the text, (b) the theoretical time dependence of $[P]$ (the reduced substrate) as shown in eq 11, (c) the fitted curve obtained from simultaneous equations of eqs 10 and 11, and (d) the experimental curve at $[E']_0 = 27 \text{ nM}$ and $[S]_0 = 620 \pm 20 \text{ ng cm}^{-2}$ on a QCM.

$$[P] = \frac{k_{\text{cat}}}{D_p} \int [E'S] dt \quad (11)$$

$$\tau^{-1} = k_{\text{on}}[E']_0 + k_{\text{off}} \quad (12)$$

The curves (a) and (b) in Figure 5B are theoretical curves from eqs 10 and 11, respectively. The curves (c) and (d) are the fitted curves obtained from the simultaneous equations both of eqs 10 and 11, and the experimental curve at $[E']_0 = 27 \text{ nM}$ and $[S]_0 = 620 \text{ ng cm}^{-2}$ on the QCM, respectively. When relaxation rates (τ^{-1}) were plotted against the concentration of AMP-activated enzyme, k_{on} and k_{off} values obtained from the linear plot of eq 12. The dissociation constant (K_d) of enzyme and amylopectin is obtained from $k_{\text{off}}/k_{\text{on}}$. Phosphorolysis rates (k_{cat}) were obtained from the fitting of eq 11. These kinetic parameters are summarized in Table 1. When the QCM technique was employed for amylopectin phosphorolysis, all kinetic parameters both of enzyme binding (k_{on} , k_{off} , and K_d) and phosphorolysis (k_{cat}) could be obtained simultaneously on the same device.

Discussion

Phosphorolysis of amylopectin by phosphorylase b from rabbit muscle was directly monitored by the QCM method, in which the formation and dissociation of the ES complex was followed as mass changes. In general, enzyme reactions have

been followed by the product formation because it was difficult to detect directly the *ES* complex concentration in the bulk solution.

Kinetic studies of amylopectin cleavage reactions by both inactivated and AMP-activated phosphorylase *b* were examined. When inactivated phosphorylase *b* was employed, three steps, including (1) binding of the inactivated enzyme to amylopectin (mass increase), (2) activation of the enzyme by AMP, and (3) phosphorolysis of α -1,4 glucosidic linkages of amylopectin (mass decrease), could be monitored as two steps (method A, Figures 2A and 3A). In the case of AMP-activated phosphorylase *b*, a total continuous step of (1) binding of the AMP-activated enzyme to amylopectin (mass increase) and (2) phosphorolysis of substrate (mass decrease) could be observed as a one step reaction (method B, Figures 2B and 5A).

All kinetic parameters obtained from methods A and B are summarized in Table 1. Dissociation constant (K_d) of AMP-activated enzyme from amylopectin was ca. 10 times smaller than that of the inactivated enzyme (1.4 nM and 12 nM, respectively). This is mainly because AMP-activated phosphorylase *b* has a ca. 40 times lower dissociation rate constant ($k_{\text{off}} = 5.0 \times 10^{-5} \text{ s}^{-1}$) than that of the inactivated enzyme ($k_{\text{off}} = 1.9 \times 10^{-3} \text{ s}^{-1}$). Thus, AMP activation of phosphorylase *b* is more effective at decreasing the dissociation rate constant (k_{off}) than increasing the binding rate constant (k_{on}) to amylopectin.

The phosphorolysis reaction is started by activated-phosphorylase *b*. In method A, the *ES* complex is first formed and then phosphorolysis is triggered by the addition of AMP. The k_{cat} values obtained both from the initial slope of Figure 3A by changing enzyme concentrations and from Lineweaver–Bulk plot (eq 9 and Figure 4C) by changing AMP concentrations were similar with each other (21 and 12 s^{-1} , respectively). In addition, k_{cat} value of AMP-activated enzyme obtained from the simultaneous equations of 10 and 11 (method B) also gave a similar k_{cat} value (18 s^{-1}). This result indicates that the inactivated enzyme could be activated by the addition of AMP and shows the same activity as the AMP-activated enzyme. The dissociation constant for AMP (K_{AMP}) was found to be $1.0 \times 10^{-4} \text{ M}$, and this is a reasonable value as the dissociation constant for small substrates. The K_{AMP} obtained from the QCM method was consistent with previous determination using a radio-isotope method in the bulk solution ($K_{\text{AMP}} = 1.2 \times 10^{-4} \text{ M}$).²¹

Michaelis–Menten kinetics have been applied to obtain both the Michaelis constant (K_m) and the catalytic rate constant (k_{cat}) according to eq 13. If $k_{\text{off}} \gg k_{\text{cat}}$, the K_m value is thought to be

the apparent dissociation constant ($K_d = k_{\text{off}}/k_{\text{on}}$).^{8,9}

$$K_m = \frac{k_{\text{off}} + k_{\text{cat}}}{k_{\text{on}}} \quad (13)$$

In the Michaelis–Menten kinetics of phosphorylase *b* for amylopectin, $K_m = 2.0 \times 10^{-6} \text{ M}$ and $k_{\text{cat}} = 24 \text{ s}^{-1}$ was previously obtained (Table 1).^{19,20} Catalytic rate constants ($k_{\text{cat}} = 12\text{--}21 \text{ s}^{-1}$) obtained from the QCM method were relatively consistent with $k_{\text{cat}} = 24 \text{ s}^{-1}$ obtained from Michaelis–Menten kinetics in the bulk solution. The dissociation constants, however, were 10^3 times different from each other ($K_d = 1.4 \times 10^{-9} \text{ M}$ from the QCM method and $K_m = 2.0 \times 10^{-6} \text{ M}$ from the Michaelis–Menten kinetics method). In the Michaelis–Menten equation, the K_m value corresponds to the dissociation constant only when $k_{\text{off}} \gg k_{\text{cat}}$. However, from the QCM experiment the value of $k_{\text{off}} = 5.0 \times 10^{-5} \text{ s}^{-1}$ was small compared with $k_{\text{cat}} = 18 \text{ s}^{-1}$. Thus, in the case of the amylopectin phosphorolysis by phosphorylase *b*, the K_m value may reflect $k_{\text{cat}}/k_{\text{on}}$ value, but not the dissociation constant (K_d). The K_d value obtained from $k_{\text{off}}/k_{\text{on}}$ by the QCM method reflects the real dissociation constant. We have recently studied the catalytic hydrolysis of amylopectin by glucoamylase using amylopectin-immobilized QCM.¹⁸ In this case, the similar kinetic parameters such as the binding and dissociation rate constants, the dissociation constant of glucoamylase to amylopectin, and the catalytic rate constant of hydrolysis were determined to be $k_{\text{on}} = 2.3 \times 10^4 \text{ M}^{-1} \text{ s}^{-1}$, $k_{\text{off}} = 9.3 \times 10^{-5} \text{ s}^{-1}$, $K_d = 4.0 \times 10^{-9} \text{ M}$, and $k_{\text{cat}} = 93 \text{ s}^{-1}$, respectively. From the Michaelis–Menten equation of the same reaction in the bulk solution, K_m and k_{cat} values were determined to be $5.9 \times 10^{-5} \text{ M}$ and $k_{\text{cat}} = 40 \text{ s}^{-1}$, respectively.²² The $K_d = 4.0 \times 10^{-9} \text{ M}$ obtained from $k_{\text{off}}/k_{\text{on}}$ using the QCM method was again largely 10^4 times different from the $K_m = 5.9 \times 10^{-5} \text{ M}$ obtained from Michaelis–Menten kinetics in the bulk solution, due to the similar reason of $k_{\text{cat}} \gg k_{\text{off}}$. Thus, in these enzyme reactions, enzymes slowly bind to substrate and proceed to phosphorolysis or hydrolysis without releasing from substrate ($k_{\text{cat}} \gg k_{\text{off}}$). Therefore, it is important to grasp all kinetic parameters such as k_{on} , k_{off} , K_d , and k_{cat} on the one device in the enzyme reactions.

In conclusion, phosphorylase *b* can bind strongly to the amylopectin substrate even as the inactivated form, and the enzyme is activated promptly by the addition of AMP leading to phosphorolysis of α -1,4 linkages of amylopectin. This is the first example of simultaneous detection of the binding and catalysis of phosphorylase *b* reactions in situ on the same device. We believe that the QCM system is a highly sensitive method of detection for in situ enzyme reactions on a α -glucan without any labeling. This system will be applicable to other polysaccharide enzyme reactions such as glycohydrolyses and transglycosylations.

JA046583K

(22) Abe, J.; Nagano, H.; Hizukuri, S. *J. Appl. Biochem.* **1985**, *7*, 235–247.

(19) Fukui, T.; Shimomura, S.; Nakano, K. *Mol. Cell. Biochem.* **1982**, *42*, 129–144.

(20) Druceckers, P.; Boeck, B.; Palm, D.; Schingel, S. *Biochemistry*, **1996**, *35*, 6727–6730.

(21) Vandebunder, B.; Dreyfus, M.; Buc, H. *Biochemistry* **1978**, *17*, 4153–4160.